Transverse single-spin asymmetries of midrapidity π^0 and η mesons in polarized $p+p$ collisions at $\sqrt{s} = 200$ GeV

PHENIX Collaboration Author List (Brant will insert later)

(Dated: November 9, 2020)

We present a measurement of the transverse single-spin asymmetry (TSSA) for π^0 and η mesons in $p^{\uparrow}+p$ collisions in the pseudorapidity range $|\eta| < 0.35$ and at a center-of-mass energy of 200 GeV with the PHENIX detector at the Relativistic Heavy Ion Collider. In comparison with previous measurements in this kinematic region, these results have a factor of 3 smaller uncertainties. As hadrons, π^0 and η mesons are sensitive to both initial- and final-state nonperturbative effects for a mix of parton flavors. Comparisons of the differences in their TSSAs have the potential to disentangle the possible effects of strangeness, isospin, or mass. These results can constrain the twist-3 trigluon collinear correlation function as well as the gluon Sivers function.

I. INTRODUCTION

The transverse structure of the proton has attracted increasing experimental and theoretical interest in the past two decades. In particular, transverse single-spin asymmetries (TSSAs) have been one of the primary means to probe transverse partonic dynamics in the nucleon. Large azimuthal asymmetries of up to $\sim 40\%$ have been observed from transversely polarized $p^{\uparrow}+p$ collisions in light meson production at large Feynman-x ($x_F = 2p_L/\sqrt{s}$), from center of mass energies of $\sqrt{s} = 4.9$ GeV up to 500 GeV [1–6]. Next-to-leading order perturbative QCD calculations that only include spin-momentum correlations from parton scattering predict small asymmetries on the order of m_q/Q [7] where m_q is the bare quark mass and Q is the hard scale, indicating that significant nonperturbative effects must dominate the large measured asymmetries. Two different approaches have been proposed to describe the large asymmetries observed in hadronic interactions.

In the first approach, nonperturbative parton distribution functions (PDFs) and fragmentation functions (FFs) are explicitly dependent on transverse momentum. In this so-called transverse-momentum-dependent (TMD) framework, these functions depend on a soft (k_T) and hard (Q) momentum scale such that $\Lambda_{QCD} \lesssim k_T \ll Q$. One possible origin of the large TSSAs is the Sivers TMD PDF [8], which correlates the nucleon transverse spin with the parton transverse momentum, k_T. Recently, this function has received great theoretical and experimental interest due to the prediction of modified universality between semi-inclusive deep-inelastic lepton-nucleon scattering (SIDIS) and the Drell-Yan (DY) process of quark-antiquark annihilation to dileptons. This prediction is a result of differences in color flow from interactions with remnants in the initial versus final states, related to the PT-odd nature of the Sivers TMD PDF and the PT invariance of QCD [9]. Another possible origin of the TSSA is the Collins TMD FF [10], which correlates the transverse polarization of a fragmenting quark to the angular distribution of hadrons.

The second approach to describe the large asymmetries relies on collinear higher-twist effects with multiparton correlations. In the twist-3 approach, interference arises between scattering amplitudes with one and two collinear partons, which leads to a nonzero TSSA. This approach applies to observables in which only one sufficiently large momentum scale (Q) is measured, such that $Q \gg \Lambda_{QCD}$. [11] In order to keep the multiparton correlation functions process-independent, the initial- and final-state interactions between the struck parton and the proton remnants are included in the hard perturbative part of the twist-3 collinear factorization [12]. Collinear twist-3 correlation functions are split into two types: the quark-gluon-quark functions (qgq) and the trigluon functions (ggg). In the context of initial-state effects, the qgq functions describe the interference from scattering off of one quark versus scattering off of a gluon and a quark of the same flavor, while the ggg functions capture the interference between scattering off of one gluon versus scattering off of two. The twist-3 approach is well suited to describe observed inclusive forward hadron asymmetries because the observed hadron p_T can be used as a proxy for the hard scale, and unlike the TMD approach, these correlation functions do not explicitly depend on a soft-scale transverse momentum. However, the twist-3 approach has been related to k_T moments of TMD PDFs and TMD FFs and has been shown to be equivalent to the TMD approach in the overlapping kinematic regime [13].

Both SIDIS and DY measurements have shown that certain TMD PDFs are consistent with modified universality provided that effects from TMD evolution with the hard-scale Q are small [14, 15] and that interactions in the initial or final state can produce nonzero asymmetries [16–19]. In hadronic interactions where at least one final-state hadron is measured, both initial- and final-state interactions can play competing roles in the measured asymmetries; here TMD-factorization breaking has been predicted due to soft gluon exchanges that are possible in both the initial and final states simultaneously [20]. Additional leading-power spin asymmetries have been predicted in hadronic collisions due to this breakdown, without which these asymmetries would be subleading [21], but further work is needed to connect TMD-factorization breaking to experimentally measured asymmetries. It is interesting to note that inclusive hadron TSSA measurements in hadronic collisions appear to plateau at p_T up to 5 GeV/c [3, 5] and have been measured to be nonzero at up to $p_T \sim 7$ GeV/c [6, 22]. Recent studies in the twist-3 framework have successfully described the p_T dependence of these forward asymmetries by including twist-3 effects in hadronization [23]. The twist-3 perturbative prediction is that the asymmetry should eventually decrease as the hard scale p_T continues increasing [21].

Since the inception of the collinear twist-3 and TMD factorization pictures, there has been theoretical evidence that they could combine to form a unified picture of TSSAs in hard processes. This concept was recently tested with the first simultaneous global analysis of TSSAs in SIDIS, DY, e^+e^- annihilation, and proton-proton collisions [11]. This study used quark TMD PDFs and FFs to describe the asymmetries in processes that are sensitive to the soft-scale momentum, i.e. SIDIS, Drell-Yan, and e^+e^- annihilation. These TMD functions were also used to calculate collinear twist-3 qgq correlation functions which were applied to inclusive forward pion asymmetry measurements from RHIC. This simultaneous description of TSSAs across multiple collision species indicates that all TSSAs have a common origin that is related to multiparton correlations.

Additional questions about the origin of the TSSAs in hadronic interactions remain. Forward jet measurements indicate that the TSSA is significantly smaller than neutral pion asymmetries at similar x_F and $\sqrt{s}$ [24]. Nonzero kaon and antiproton asymmetries observed at forward rapidities show that the measured asymmetries cannot be due only to proton valence quark contributions as naively predicted in a valence-like model, where the Sivers effect from sea-quarks and/or gluons is ignored, and that the fragmentation of quarks into hadrons in which they are not valence quarks could play a role in the observed nonzero asymmetries [4, 25]. Eta meson measurements, sensitive to potential effects from strange quark contributions, isospin, and/or hadron mass show forward asymmetries similar in magnitude to neutral pions [26]. Even four decades after the initial discovery of large TSSAs in hadronic interactions [1], there remain many unresolved questions about their origin. Therefore it is crucial to continue extending measurements to try to better understand the nonperturbative dynamics which are responsible for the TSSAs in hadronic collisions.

In this paper we report a measurement of the TSSA of π^0 and η mesons in $p^\uparrow$+p collisions at $\sqrt{s} = 200$ GeV in the midrapidity region $|\eta| < 0.35$. The data was taken during the 2015 RHIC run and a total integrated luminosity of approximately 60 pb^{-1} was collected. This measurement extends previous measurements from RHIC to higher p_T and reduces the statistical uncertainties by a factor of three in the overlapping p_T region.

II. ANALYSIS

The asymmetries are measured with transversely polarized proton beams where the average polarization of the clockwise beam was 0.58 ± 0.02 and that of the counter-clockwise beam was 0.60 ± 0.02 [27]. The direction of the beam polarization was found to be consistent with the vertical within statistical uncertainties. The polarization direction of each beam independently changes bunch to bunch which reduces systematic uncertainties associated with variations in detector performance with time. It also allows for polarization-averaged measurements and, for a single-spin asymmetry analysis, means there are two ways to measure the TSSA with the same data set. This is done by sorting the particle yields for the polarization directions of one beam at a time, effectively averaging over the polarization of the other beam. These statistically independent asymmetries are used to verify the analysis and are averaged together for the final result.

The data analysis procedure is similar to our previous measurements [5]. Neutral pion and eta mesons are reconstructed via their two-photon decays by using the midrapidity electromagnetic calorimeter (EMCal). The EMCal is located in two central arms, each covering $\Delta\phi = \pi/2$ in azimuth and $|\eta| < 0.35$ in pseudorapidity, centered at $\phi = \pi/16$ and $15\pi/16$. It is comprised of two different types of calorimeters: six sectors of sampling lead-scintillator (PbSc) calorimeters and two sectors of Cherenkov lead-glass (PbGl) calorimeters [28]. The two calorimeter systems have different granularity ($\delta\phi \times \delta\eta = 0.011 \times 0.011$ in the PbSc and 0.008×0.008 in the PbGl) and also different responses to charged hadrons, which provides important systematic cross checks for these measurements. A tracking system includes a drift chamber to measure track momentum and pad chamber stations to measure the charged particle hit position [29]. The measurement of the track positions in front of the calorimeter is used to veto charged particles from the photon sample. The Beam-Beam Counters (BBC) are arrays of quartz Cherenkov radiators that surround the beam pipe and are placed ± 144 cm away from the nominal collision point. The BBC covers full azimuth and $3.0 < |\eta| < 3.9$ in pseudorapidity. They measure the z-vertex position; a vertex cut of ± 30 cm around the nominal collision point is used for this analysis. The minimum bias trigger requires at least one charged particle to be measured in both the north and south sides of the BBC. This analysis is based on the data sample selected with the EMCal-based high-energy-photon trigger with energy threshold of 1.5 GeV, which is taken in coincidence with the minimum bias trigger.

Photons are identified as clusters in the EMCal and are required to pass a shower profile cut which suppresses clusters from hadrons. High-p_T trigger photons are paired with another photon in the same event that is also on the same side of the detector. A charged track veto cut eliminates clusters that geometrically match with a measured charged track, reducing background from electrons. The contribution of EMCal detector noise is reduced by a minimum energy cut of 0.5 GeV and a time-of-flight cut of $|TOF| < 5$ ns. The timing of the cluster is measured by the EMCal and the time zero reference of the event is provided by the BBC. Each photon pair is required to pass an energy asymmetry cut: $\alpha = |E_1 - E_2|/(E_1 + E_2) < 0.8$. π^0 yields are comprised of photon pairs with invariant mass in the signal region ± 25 MeV/c^2 from the π^0 mass peak and η meson yields are measured in the range ± 70 MeV/c^2 around the η mass peak.

The transverse single-spin asymmetries are determined with the "relative luminosity" formula

$$A_N = \frac{1}{P\ \langle\cos(\phi)\rangle}\frac{N^{\uparrow} - \mathcal{R}N^{\downarrow}}{N^{\uparrow} + \mathcal{R}N^{\downarrow}}, \tag{1}$$

which compares the yield of particles for when the beam was polarized up versus down. Here P is the beam polarization, N refers to the meson yield, and the arrows refer to the up ($\uparrow$) or down ($\downarrow$) directions of beam polarization. The relative luminosity, $\mathcal{R} = \mathcal{L}^{\uparrow}/\mathcal{L}^{\downarrow}$, is the ratio of the integrated luminosity with bunches that were polarized in opposite directions. This is determined by the number of times each crossing fires the minimum bias trigger and is measured to better than 10^{-4}. The acceptance factor, $\langle\cos(\phi)\rangle$, accounts for the detector azimuthal coverage, where $\phi = 0$ points 90° from the (vertical) spin axis. This correction is calculated as a function of photon pair p_T because the diphoton azimuthal acceptance depends heavily on the decay angle and ranges from 0.95 at low p_T to 0.89 at high p_T. The asymmetry is calculated separately for the two detector arms and then the average weighed by the statistical error is taken for the final result. Eq. (1) as written is for the arm to the left of the beam taken as polarized, while an overall minus sign is needed for the arm to the right of the beam taken as polarized.

An alternative method of calculating the asymmetry is the "square root" formula

$$A_N = \frac{1}{P\ \langle\cos(\phi)\rangle}\frac{\sqrt{N_L^{\uparrow}N_R^{\downarrow}} - \sqrt{N_L^{\downarrow}N_R^{\uparrow}}}{\sqrt{N_L^{\uparrow}N_R^{\downarrow}} + \sqrt{N_L^{\downarrow}N_R^{\uparrow}}}, \tag{2}$$

which is used as a cross check. This formula combines data from the two arms (left and right) and both beam polarization directions (up and down). The subscripts in Eq. (2) refer to the yields to the left (L) and right (R) side of the polarized beam momentum direction.

The measured asymmetries are also corrected for background

$$A_N^{\mathrm{Sig}} = \frac{A_N - r\cdot A_N^{\mathrm{BG}}}{1-r}, \tag{3}$$

where r is the fractional contribution of photon pairs from combinatorial background within the invariant mass peak. The background fraction is calculated from fits to the invariant mass spectra where a Gaussian is used to describe the invariant mass peak, and a third order polynomial is used to describe the combinatorial background, as shown in the green curves in Figure 1. Using this method, the contribution of combinatorial background under the π^0 peak is determined to vary from 10% in the lowest p_T bin to 6% in the highest. Under the η meson invariant mass peak, the background fraction varies from 71% to 47% in the lowest to highest p_T bins. In Eq. (3), the background asymmetry, A_N^{BG}, is evaluated with photon pairs in side band regions located on either side of the signal peak, as represented in the red regions in Figure 1. For the π^0 analysis these side band regions are $47 < M_{\gamma\gamma} < 97$ MeV/c^2 and $177 < M_{\gamma\gamma} < 227$ MeV/c^2, and for the η meson analysis these regions are $300 < M_{\gamma\gamma} < 400$ MeV/c^2 and $700 < M_{\gamma\gamma} < 800$ MeV/c^2. The background asymmetries are consistent with zero across all p_T bins.

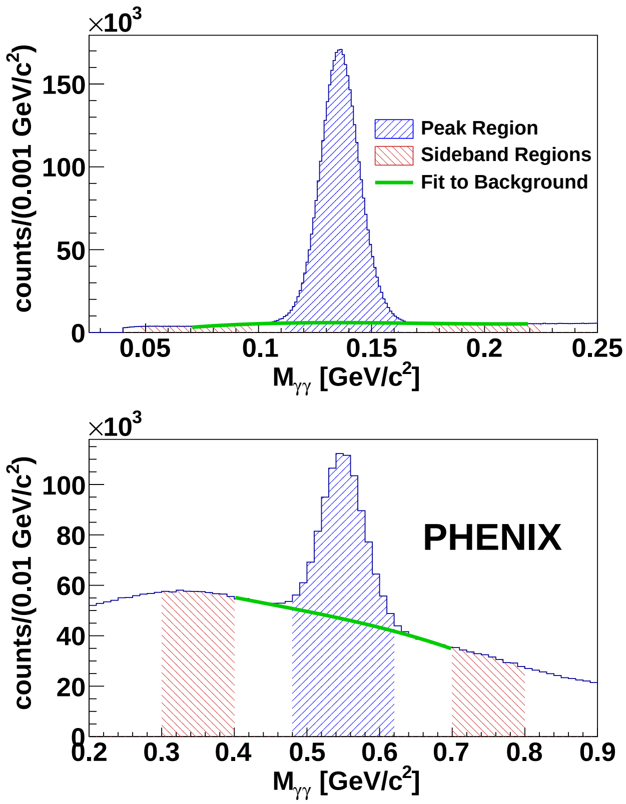

FIG. 1. Example invariant mass distributions around the π^0 (top) and η (bottom) peak for photon pairs with $4 < p_T < 5$ GeV/c in one of the detector arms. The blue region at the center of each plot corresponds to the invariant mass region under the peak which is used to calculate A_N in Eq. (3) and the red side band regions correspond to the photon pairs that are used to calculate A_N^{BG}. The green curve corresponds to the fit to the combinatorial background which is used to calculate the background fraction.

A summary of the asymmetries and statistical and systematic uncertainties can be found in Tables I and II where the total systematic uncertainty is the sum of the three sources of systematic uncertainty added in quadrature. The systematic uncertainty on the asymmetry due to the background fraction in Eq. (3) is determined by varying the fit ranges when computing r and calculating how much the background-corrected asymmetry changes. While the asymmetries calculated with the "relative luminosity" (Eq. (1)) and the "square root" (Eq. (2)) formulas were found to be statistically consistent, their difference was assigned as a systematic uncertainty due to possible variations in detector performance and beam conditions. This dominates the total systematic uncertainty for most p_T bins.

Bunch shuffling is a technique used to investigate potential sources of systematic uncertainty that could cause the measured asymmetry results to vary from their true values beyond statistical fluctuations. It involves randomizing the assigned bunch-by-bunch polarization directions of the beam such that the physical asymmetry disappears in order to isolate the statistical variations present in the data. All asymmetry values have bunch shuffling results consistent with statistical variations except for the lowest p_T bin where there is 7% and 6% more variation beyond what is expected from statistical fluctuations in the π^0 and η meson analyses, respectively. These values are used to assign additional systematic uncertainties to the lowest p_T bin of the π^0 and η meson asymmetries and dominate the total systematic uncertainty for those bins.

Additional cross checks included examining the asymmetries in the two arms separately using Eq. (1) and measuring the asymmetry as an explicit function of ϕ. All checks were statistically consistent with the main asymmetry results.

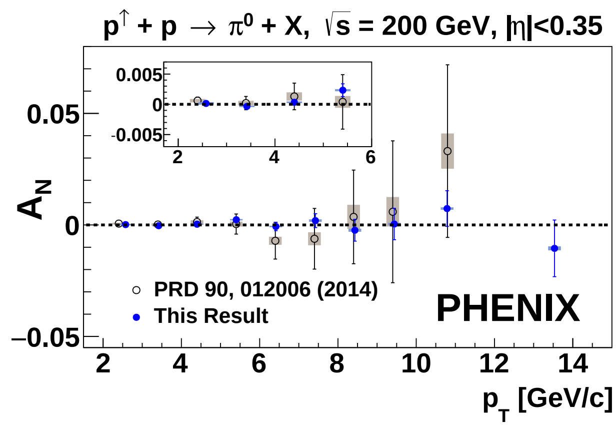

FIG. 2. Transverse single-spin asymmetry of neutral pions measured at $|\eta| < 0.35$ in $p^{\uparrow}$+p collisions at $\sqrt{s} = 200$ GeV. An additional scale uncertainty of 3.4% due to the polarization uncertainty is not shown.

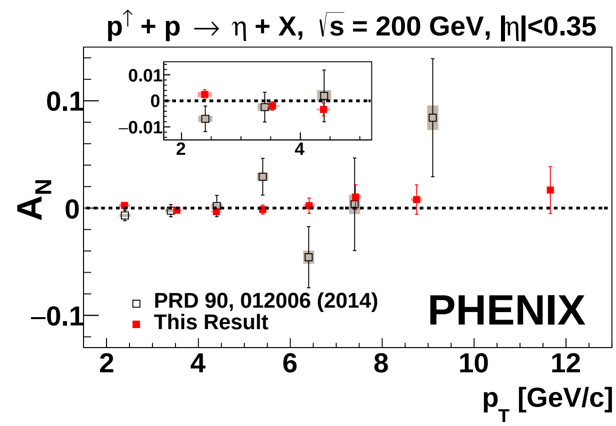

FIG. 3. Transverse single-spin asymmetry of eta mesons measured at $|\eta| < 0.35$ in $p^{\uparrow}$+p collisions at $\sqrt{s} = 200$ GeV. An additional scale uncertainty of 3.4% due to the polarization uncertainty is not shown.

III. RESULTS AND DISCUSSION

The result for A_N of neutral pions at midrapidity in $p^{\uparrow}$+p collisions at $\sqrt{s} = 200$ GeV is shown in Figure 2 where the bands represent the systematic uncertainty and the bars represent the statistical uncertainty. The figure shows this result compared to the previous results [5], demonstrating the improvement in statistical precision. In Figure 2, the inset shows a zoomed-in comparison at small p_T. The new measurement is consistent with our previous measurement and improves the precision on average by a factor of 3. The new measurement of A_N of neutral pions is consistent with zero in the entire p_T range.

The measurement of A_N of η mesons in $p^{\uparrow}$+p collisions at $\sqrt{s} = 200$ GeV is shown in Figure 3. This measurement is also compared to the previous result, similarly to Figure 2. The new measurement is consistent with the previous result and with zero across the entire p_T range. Comparisons of π^0 and η meson TSSAs may indicate additional effects from strange quarks, isospin differences, or hadron mass. At forward rapidity, existing measurements [26, 30] do not yet clearly resolve whether the η meson asymmetry is larger than the π^0 asymmetry as predicted in some models [31]. At midrapidity, there is a larger contribution from gluon dynamics and, as shown in Figure 4, both asymmetries are consistent with zero and therefore show no evidence for differences due to strangeness, isospin, or mass.

Figure 5 shows this π^0 TSSA result plotted with theoretical predictions. The qgq curve shows the predicted contribution from collinear twist-3 qgq functions from both the polarized proton and the process of hadronization. This curve was calculated with fits that were published in Ref. [11] and has been reevaluated in the rapidity range of PHENIX. Midrapidity π^0 production includes a large fractional contribution from gluons in the proton, so a complete collinear twist-3 description of the midrapidity π^0 TSSA would also need to include the contribution from the trigluon correlation function. Given

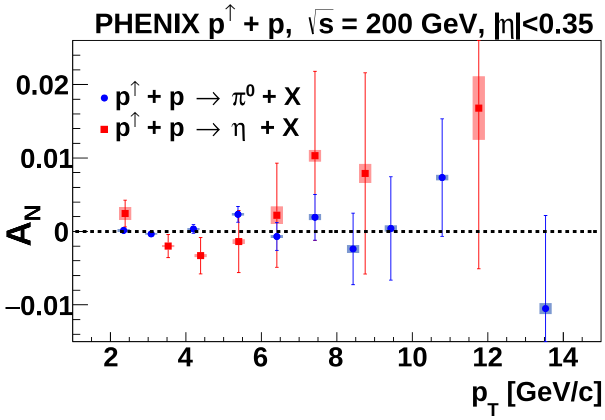

FIG. 4. Comparison of the π^0 and η meson asymmetries measured at $|\eta| < 0.35$ in $p^{\uparrow}+p$ collisions at $\sqrt{s} = 200$ GeV. An additional scale uncertainty of 3.4% due to the polarization uncertainty is not shown.

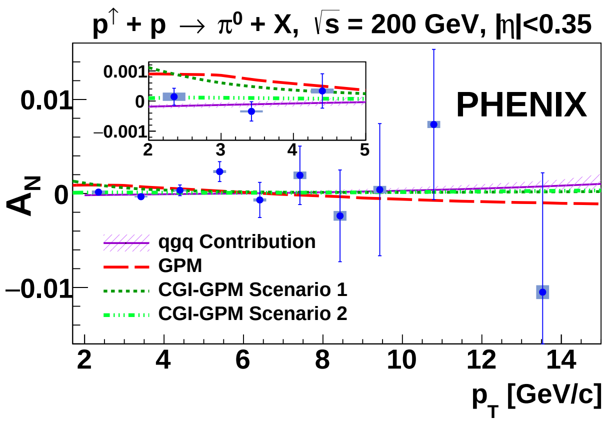

FIG. 5. This π^0 asymmetry result plotted with theory calculations for the asymmetry in both the collinear twist-3 [11] and TMD [32] theoretical frameworks. See text for details.

the small expected contribution from the qgq correlation function, this measurement can constrain future calculations of the ggg correlation function, such as those in Ref. [33].

The other theory curves in Figure 5 show predictions for the midrapidity π^0 TSSA generated by the Sivers TMD PDF. These curves include contributions from both the quark and gluon Sivers functions and have been evaluated for $x_F = 0$, which approximates the measured kinematics. These calculations use the generalized parton model (GPM) which takes the first k_T moment of the Sivers function (e.g. $\int k_T \cdot q(k_T)$) and does not include next-to-leading-order (NLO) interactions with the proton fragments. The "GPM" curve uses the parameters stated in Equation 32 of Ref. [32]. The color-gauge-invariant generalized parton model (CGI-GPM) expands on the GPM by including initial- and final-state interactions through the one-gluon exchange approximation. This model has been shown to reproduce the predicted sign change for the quark Sivers function in SIDIS and Drell-Yan. The CGI-GPM curves plotted in Figure 5 show two different scenarios for this model, the specifics of which can be found in Equation 34 of Ref. [32]. The values that are used for the Scenario 1 curve are chosen to maximize the open heavy flavor TSSA generated by the gluon Sivers function while still keeping this asymmetry within the statistical error bars of the published result in Ref. [34] and simultaneously describing the previously published midrapidity π^0 TSSA from Ref. [5]. The values used in the Scenario 2 curve are similarly calculated, except that they minimize the open heavy flavor TSSA within the range of the published statistical error bars. As shown in the zoomed-in inset of Figure 5, this π^0 TSSA result has the statistical precision at low p_T needed to distinguish between the GPM and CGI-GPM frameworks, preferring CGI-GPM Scenario 2.

Measurements of TSSAs in p+p collisions are essential to understanding the underlying nonperturbative processes which generate them. In particular, further measurements are necessary to clarify certain questions in the interpretations of the TSSAs. For example, the small forward jet asymmetries measured in Ref. [24] have been interpreted as a cancellation of up and down quark asymmetries, implying that the comparatively forward large neutral pion asymmetries include significant contributions from spin-momentum correlations in hadronization [23]. Additionally, the p_T dependence of these forward rapidity measurements remains to be clearly understood; measurements of nonzero asymmetries out to even higher p_T would help confirm that these twist-3 observables eventually fall off with increasing hard scale. While the midrapidity measurements here are all consistent with zero, they still provide the highest available statistical precision and p_T reach available at the PHENIX experiment. While forward rapidity light hadron TSSAs are dominated by valence quark spin-momentum correlations in the polarized proton, these midrapidity TSSA measurements are sensitive to both quark and gluon dynamics at leading order. Thus these data also provide further constraints to gluon spin-momentum correlations in transversely polarized protons [33, 35].

IV. SUMMARY

The measurements presented here were motivated by the outstanding questions regarding the physical origin of TSSAs. The TSSAs of π^0 and η mesons were measured at midrapidity in p+p collisions at $\sqrt{s} = 200$ GeV by the PHENIX experiment. The measured π^0 (η meson) asymmetry is consistent with zero in the presented p_T range, up to precision of 3×10^{-4} (2×10^{-3}) in the lowest p_T bins. Both measurements have a significant reduction in uncertainty from previous measurements at midrapidity at RHIC. These data extend previous constraints to any presence of gluon spin-momentum correlations in transversely polarized protons.

TABLE I. The measured A_N of π^0 in p+p collisions at $\sqrt{s}$ =200 GeV as a function of p_T. An additional scale uncertainty of 3.4% due to the polarization uncertainty is not shown. The total $\sigma_{\rm syst}$ in the lowest p_T bin includes an additional systematic uncertainty of 1.06×10^{-4} from bunch shuffling.

$\langle p_T \rangle$(GeV/c)	A_N	$\sigma_{\rm stat}$	$\sigma_{\rm syst}$ (rel. lumi. vs sqrt.)	$\sigma_{\rm syst}$ (bg. fraction)	$\sigma_{\rm syst}$ (total)
2.58	1.43×10^{-4}	2.81×10^{-4}	5.71×10^{-5}	3.92×10^{-7}	1.20×10^{-4}
3.42	-3.43×10^{-4}	3.21×10^{-4}	1.73×10^{-5}	3.92×10^{-6}	1.77×10^{-5}
4.40	3.35×10^{-4}	5.71×10^{-4}	6.56×10^{-5}	1.91×10^{-6}	6.57×10^{-5}
5.40	2.33×10^{-3}	1.06×10^{-3}	9.61×10^{-5}	6.68×10^{-7}	9.61×10^{-5}
6.41	-6.89×10^{-4}	1.87×10^{-3}	1.12×10^{-4}	2.11×10^{-5}	1.14×10^{-4}
7.42	1.93×10^{-3}	3.11×10^{-3}	3.41×10^{-4}	7.61×10^{-5}	3.50×10^{-4}
8.43	-2.38×10^{-3}	4.88×10^{-3}	2.45×10^{-4}	3.99×10^{-4}	4.69×10^{-4}
9.43	4.04×10^{-4}	7.03×10^{-3}	3.31×10^{-4}	1.16×10^{-4}	3.51×10^{-4}
10.79	7.34×10^{-3}	7.99×10^{-3}	9.71×10^{-5}	3.13×10^{-4}	3.28×10^{-4}
13.53	-1.05×10^{-2}	1.27×10^{-2}	6.86×10^{-4}	1.15×10^{-5}	6.86×10^{-4}

TABLE II. The measured A_N of η mesons in p+p collisions at $\sqrt{s}$ =200 GeV as a function of p_T. An additional scale uncertainty of 3.4% due to the polarization uncertainty is not shown. The total $\sigma_{\rm syst}$ in the lowest p_T bin includes an additional systematic uncertainty of 6.20×10^{-4} from bunch shuffling.

$\langle p_T \rangle$(GeV/c)	A_N	$\sigma_{\rm stat}$	$\sigma_{\rm syst}$ (rel. lumi. vs sqrt.)	$\sigma_{\rm syst}$ (bg. fraction)	$\sigma_{\rm syst}$ (total)
2.39	2.44×10^{-3}	1.83×10^{-3}	5.18×10^{-4}	4.58×10^{-5}	8.09×10^{-4}
3.53	-1.99×10^{-3}	1.59×10^{-3}	8.36×10^{-5}	3.31×10^{-5}	8.99×10^{-5}
4.39	-3.31×10^{-3}	2.48×10^{-3}	1.44×10^{-4}	4.55×10^{-5}	1.51×10^{-4}
5.40	-1.39×10^{-3}	4.21×10^{-3}	2.41×10^{-4}	3.59×10^{-5}	2.44×10^{-4}
6.41	2.22×10^{-3}	7.09×10^{-3}	1.12×10^{-3}	6.35×10^{-6}	1.12×10^{-3}
7.42	1.03×10^{-2}	1.15×10^{-2}	7.03×10^{-4}	1.60×10^{-4}	7.20×10^{-4}
8.75	7.90×10^{-3}	1.37×10^{-2}	1.24×10^{-3}	1.88×10^{-4}	1.25×10^{-3}
11.76	1.68×10^{-2}	2.19×10^{-2}	4.25×10^{-3}	3.70×10^{-4}	4.26×10^{-3}

ACKNOWLEDGMENTS

[1] R. D. Klem, J. E. Bowers, H. W. Courant, H. Kagan, M. L. Marshak, E. A. Peterson, K. Ruddick, W. H. Dragoset, and J. B. Roberts, "Measurement of Asymmetries of Inclusive Pion Production in Proton Proton Interactions at 6-GeV/c and 11.8-GeV/c," Phys. Rev. Lett. **36**, 929–931 (1976).

[2] D. L. Adams *et al.* (FNAL-E704 Collaboration), "Analyzing power in inclusive π^+ and π^- production at high x_F with a 200-GeV polarized proton beam," Phys. Lett. **B264**, 462–466 (1991).

[3] B. I. Abelev *et al.* (STAR Collaboration), "Forward Neutral Pion Transverse Single Spin Asymmetries in p+p Collisions at $\sqrt{s}$ = 200 GeV," Phys. Rev. Lett. **101**, 222001 (2008).

[4] I. Arsene *et al.* (BRAHMS Collaboration), "Single Transverse Spin Asymmetries of Identified Charged Hadrons in Polarized p+p Collisions at $\sqrt{s}$ = 62.4 GeV," Phys. Rev. Lett. **101**, 042001 (2008).

[5] A. Adare *et al.* (PHENIX Collaboration), "Measurement of transverse-single-spin asymmetries for midrapidity and forward-rapidity production of hadrons in polarized p+p collisions at $\sqrt{s}$ =200 and 62.4 GeV," Phys. Rev. **D90**, 012006 (2014).

[6] S. Heppelmann, "Large p_T Forward Transverse Single Spin Asymmetries of π^0 Mesons at $\sqrt{s}$=200 and 500 GeV from STAR," POS **DIS2013**, 240 (2013).

[7] G. L. Kane, J. Pumplin, and W. Repko, "Transverse Quark Polarization in Large p_T Reactions, e^+e^- Jets, and Leptoproduction: A Test of QCD," Phys. Rev. Lett. **41**, 1689 (1978).

[8] D. W. Sivers, "Single Spin Production Asymmetries from the Hard Scattering of Point-Like Constituents," Phys. Rev. **D41**, 83 (1990).

[9] J. C. Collins, "Leading twist single transverse-spin asymmetries: Drell-Yan and deep inelastic scattering," Phys. Lett. **B536**, 43–48 (2002).

[10] J. C. Collins, "Fragmentation of transversely polarized quarks probed in transverse momentum distributions," Nucl. Phys. **B396**, 161–182 (1993).

[11] Justin Cammarota, Leonard Gamberg, Zhong-Bo Kang, Joshua A. Miller, Daniel Pitonyak, Alexei Prokudin, Ted C. Rogers, and Nobuo Sato (Jefferson Lab Angular Momentum), "Origin of single transverse-spin asymmetries in high-energy collisions," Phys. Rev. D **102**, 054002 (2020), arXiv:2002.08384 [hep-ph].

[12] S. M. Aybat, J. C. Collins, J. W. Qiu, and T. C. Rogers, "The QCD Evolution of the Sivers Function," Phys. Rev. **D85**, 034043 (2012).

[13] X. Ji, J. W. Qiu, W. Vogelsang, and F. Yuan, "A Unified picture for single transverse-spin asymmetries in hard processes," Phys. Rev. Lett. **97**, 082002 (2006).

[14] L. Adamczyk *et al.* (STAR Collaboration), "Measurement of the transverse single-spin asymmetry in $p^{\uparrow}+p \to W^{\pm}/Z^0$ at RHIC," Phys. Rev. Lett. **116**, 132301 (2016).

[15] M. Aghasyan *et al.* (COMPASS Collaboration), "First measurement of transverse-spin-dependent azimuthal asymmetries in the Drell-Yan process," Phys. Rev. Lett. **119**, 112002 (2017).

[16] A. Airapetian *et al.* (HERMES Collaboration), "Single-spin asymmetries in semi-inclusive deep-inelastic scattering on a transversely polarized hydrogen target," Phys. Rev. Lett. **94**, 012002 (2005).

[17] C. Adolph *et al.* (COMPASS Collaboration), "Collins and Sivers asymmetries in muonproduction of pions and kaons off transversely polarised protons," Phys. Lett. **B744**, 250–259 (2015).

[18] R. Seidl *et al.* (BELLE Collaboration), "Measurement of azimuthal asymmetries in inclusive production of hadron pairs in e^+e^- annihilation at Belle," Phys. Rev. Lett. **96**, 232002 (2006).

[19] J. P. Lees *et al.* (BaBar Collaboration), "Measurement of Collins asymmetries in inclusive production of charged pion pairs in $\mathrm{e}^+\mathrm{e}^-$ annihilation at BABAR," Phys. Rev. **D90**, 052003 (2014).

[20] T. C. Rogers and P. J. Mulders, "No Generalized TMD-Factorization in Hadro-Production of High Transverse Momentum Hadrons," Phys. Rev. **D81**, 094006 (2010).

[21] T. C. Rogers, "Extra spin asymmetries from the breakdown of transverse-momentum-dependent factorization in hadron-hadron collisions," Phys. Rev. **D88**, 014002 (2013).

[22] Christopher Dilks (STAR Collaboration), "Measurement of Transverse Single Spin Asymmetries in π^0 Production from $p^{\uparrow}+p$ and $p^{\uparrow}+A$ Collisions at STAR," PoS **DIS2016**, 212 (2016), arXiv:1805.08875 [hep-ex].

[23] Koichi Kanazawa, Yuji Koike, Andreas Metz, and Daniel Pitonyak, "Towards an explanation of transverse single-spin asymmetries in proton-proton collisions: the role of fragmentation in collinear factorization," Phys. Rev. D **89**, 111501 (2014), arXiv:1404.1033 [hep-ph].

[24] L. C. Bland *et al.* (AnDY Collaboration), "Cross Sections and Transverse Single-Spin Asymmetries in Forward Jet Production from Proton Collisions at $\sqrt{s} = 500$ GeV," Phys. Lett. **B750**, 660–665 (2015).

[25] J.H. Lee and F. Videbaek for the BRAHMS Collaboration, "Cross-sections and Single Spin Asymmetries of Identified Hadrons in $p^{\uparrow}+p$ at $\sqrt{s} = 200$ GeV," Proc. of XVII Int. Workshop on Deep-Inelastic Scattering and Related Topics (2009).

[26] A. Adare *et al.* (PHENIX Collaboration), "Cross section and transverse single-spin asymmetry of η mesons in $p^{\uparrow}+p$ collisions at $\sqrt{s} = 200$ GeV at forward rapidity," Phys. Rev. **D90**, 072008 (2014).

[27] W. D. Schmidke *et al.* (The RHIC Polarimetry Group), "RHIC polarization for Runs 9–17," https://technotes.bnl.gov/Home/ViewTechNote/209057 (2018).

[28] L. Aphecetche *et al.* (PHENIX), "PHENIX calorimeter," Nucl. Instrum. Meth. **A499**, 521–536 (2003).

[29] K. Adcox *et al.* (PHENIX), "PHENIX central arm tracking detectors," Nucl. Instrum. Meth. A **499**, 489–507 (2003).

[30] L. Adamczyk *et al.* (STAR), "Transverse Single-Spin Asymmetry and Cross-Section for π^0 and η Mesons at Large Feynman-x in Polarized $p+p$ Collisions at $\sqrt{s} = 200$ GeV," Phys. Rev. D **86**, 051101 (2012), arXiv:1205.6826 [nucl-ex].

[31] Koichi Kanazawa and Yuji Koike, "A phenomenological study on single transverse-spin asymmetry for inclusive light-hadron productions at RHIC," Phys. Rev. **D83**, 114024 (2011).

[32] U. D'Alesio, C. Flore, F. Murgia, C. Pisano, and P. Taels, "Unraveling the Gluon Sivers Function in Hadronic Collisions at RHIC," Phys. Rev. D **99**, 036013 (2019).

[33] H. Beppu, K. Kanazawa, Y. Koike, and S. Yoshida, "Three-gluon contribution to the single spin asymmetry for light hadron production in pp collision," Phys. Rev. D **89**, 034029 (2014).

[34] C. Aidala *et al.* (PHENIX), "Cross section and transverse single-spin asymmetry of muons from open heavy-flavor decays in polarized $p+p$ collisions at $\sqrt{s} = 200$ GeV," Phys. Rev. D **95**, 112001 (2017).

[35] U. D'Alesio, F. Murgia, and C. Pisano, "Towards a first estimate of the gluon Sivers function from A_N data in pp collisions at RHIC," JHEP **09**, 119 (2015), arXiv:1506.03078 [hep-ph].